MRS Communications (2019), 9, 229–235
© Materials Research Society, 2018
doi:10.1557/mrc.2018.201

MRS Communications

Research Letter

Polydiacetylene ribbons formed using the controlled evaporative self-assembly (CESA) method

E. Van Keuren, Department of Physics and Institute for Soft Matter Synthesis and Metrology, Georgetown University, Washington DC 20057, USA
C. Pornrungroj, and **C. Fu,** Institute of Multidisciplinary Research for Advanced Materials (IMRAM), Tohoku University, 2-1-1 Katahira, Aoba-ku, Sendai 980-8577, Japan
X. Zhang, Department of Physics and Institute for Soft Matter Synthesis and Metrology, Georgetown University, Washington DC 20057, USA
S. Okada, H. Katsuyama, and **K. Kikuchi,** Graduate School of Organic Materials Science, Yamagata University, 3-16 Jonan, Yonezawa 982-8510, Japan
T. Onodera, and **H. Oikawa,** Institute of Multidisciplinary Research for Advanced Materials (IMRAM), Tohoku University, 2-1-1 Katahira, Aoba-ku, Sendai 980-8577, Japan

Address all correspondence to E. Van Keuren at **erv@georgetown.edu**

(Received 6 July 2018; accepted 10 September 2018)

Abstract

Methods for the control of molecular deposition and orientation are critical for the development of organic electronic devices. Here, we show the fabrication of ribbons of the optical material polydiacetylene (PDA) using a controlled evaporative self-assembly method. The ability to form these ribbons is highly dependent on both the side groups on the PDA as well as the solvent used in the preparation. Arrays of ribbons of one type of PDA, poly[1,6-di(*N*-carbazolyl)-2,4-hexadiyne], with widths on the order of 1–2 μm and lengths of 100s of micrometers, could be successfully obtained with good orientation.

Introduction

There has been intense research over the past several decades on developing materials and processes for organic electronics.[1–3] While significant advances have been made in the synthesis of new materials, methods which can reliably deposit organic material at specific locations on a substrate and with controlled orientation are needed for practical development of organic electronic devices. Processes that make use of the flow during coating and drying have been shown to be effective at this, and are also attractive since they can be adapted to roll-to-roll coating methods.[4]

One such method, controlled evaporative self-assembly (CESA),[5,6] has been shown to be effective for obtaining well-aligned nano- and micro-wires of organic crystals and polymers [see Fig. 1(a)]. In this method, the crystal or polymer aligns during solvent evaporation in the presence of capillary forces. These forces arise from the meniscus of the solvent made by a glass cylinder placed on top of the drying solution, similar to the conditions that occur during dip coating.[7] CESA is similar to other methods in relying on the Marangoni flow to carry solute to a receding contact line, where it is deposited as a solid.[4]

Polydiacetylene (PDA) [Fig. 1(b)] is a well-known semiconducting polymer that has been extensively studied for its interesting optical properties, in particular its strong optical non-linearity.[8,9] It has been used to create all-optical switches[10] as well as organic field effect transistors.[11–14] PDA has the distinction of being able to be polymerized in the solid state after crystallization of the monomer.[15] Here, we make use of this property in using CESA to create ordered and oriented ribbons of diacetylene (DA) monomer followed by photopolymerization. We show that polymers synthesized from the monomer 1,6-di(*N*-carbazolyl)-2,4-hexadiyne (DCHD) can easily form ribbons, while monomers with other side groups do not. In addition, we found that the method is highly dependent on the solvent, with samples prepared from acetone solution yielding regular arrays of ribbons, while samples prepared with other solvents yielded a variety of morphologies.

Materials and methods

The chemical structures of all monomers are shown in Fig. 1(b). 10,12-Tricosadiynoic acid (TCDA) and 1,4-diphenylbutadiyne (DPBD) were purchased from TCI. DCHD was purchased from Wako Chemicals. 9-BCMU (a (butoxycarbonylmethyl)urethane derivative, 10,12-docosadiyn-1,22-diyl bis(*N*-butoxycarbonylmethyl)carbamate) was synthesized from 10-undecyn-1-ol by the following two-step procedure found in the literature.[16]

To 10-undecyn-1-ol (2.00 g, 11.9 mmol) and butyl isocyanateacetate (2.25 g, 14.3 mmol) in toluene (20 mL), three drops of dibutyltin dilaurate were added, and the mixture was stirred for 21 h at ambient temperature. Solvent of the reaction mixture was evaporated and the residue was purified by column

https://doi.org/10.1557/mrc.2018.201 Published online by Cambridge University Press

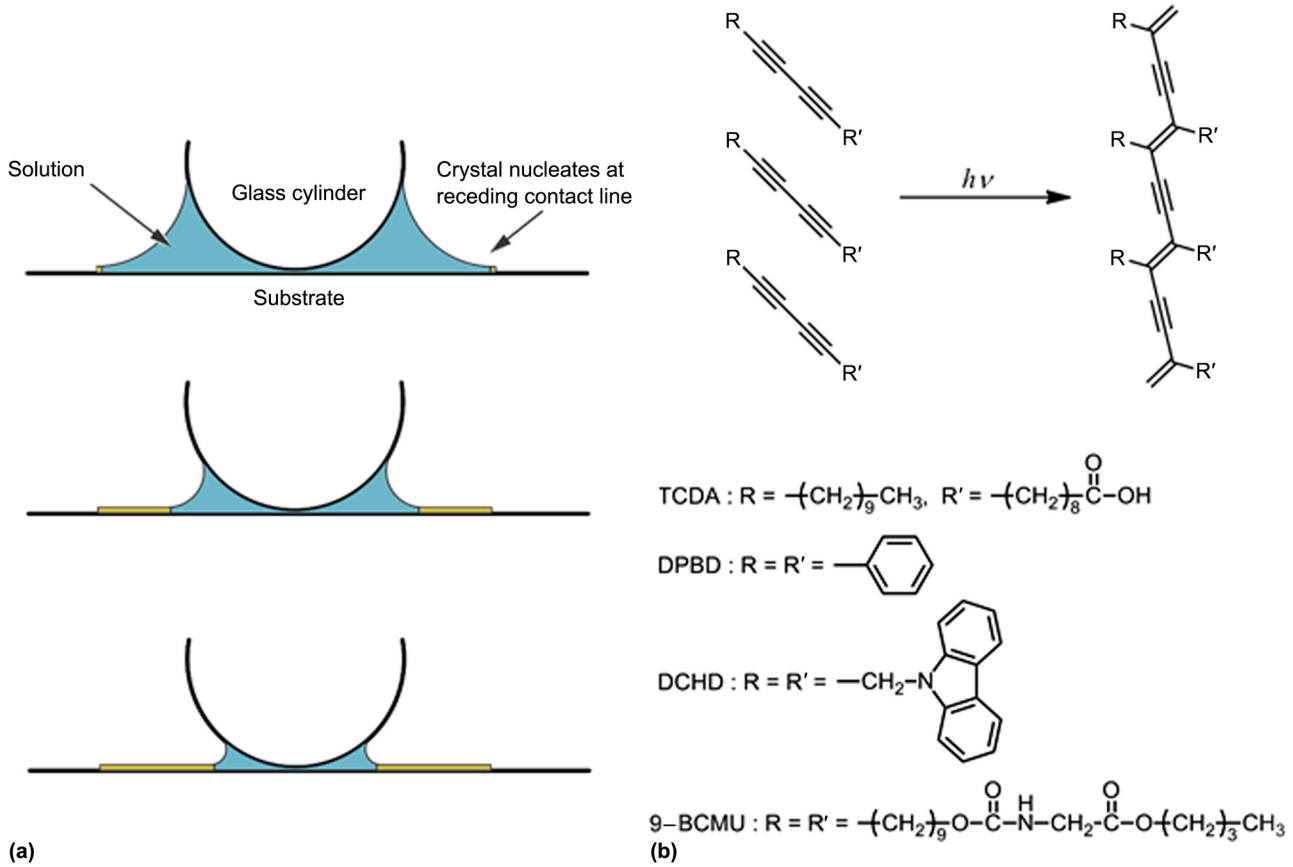


Figure 1. (a) Schematic diagram of the CESA method, (b) schematic diagram of the polymerization of polydiacetylene and chemical structure of the monomers.

chromatography (silica gel, chloroform:ethyl acetate = 9:1) to give 3.60 g (93%) of 10-undecynyl *N*-(butoxycarbonylmethyl)carbamate as colorless viscous oil. ^{1}H NMR (400 MHz, $CDCl_3$, δ) 0.93 (3H, t, J = 7.3 Hz), 1.25–1.43 (12H, m), 1.52 (2H, tt, J = 7.2, 7.2 Hz), 1.57–1.67 (4H, m), 1.95 (1H, t, J = 2.6 Hz), 2.18 (2H, td, J = 7.0, 2.6 Hz), 3.95 (2H, d, J = 5.7 Hz), 4.06 (2H, t, J = 6.6 Hz), 4.15 (2H, t, J = 6.6 Hz), 5.37 (1H, broad t); ^{13}C NMR (100 MHz, $CDCl_3$, δ) 13.48, 18.18, 18.85, 25.59, 28.26, 28.51, 28.76, 28.82, 29.01, 29.17, 30.36, 42.49, 65.06, 65.23, 67.98, 84.49, 156.55, 170.16.

10-Undecynyl *N*-(butoxycarbonylmethyl)carbamate (3.12 g, 9.59 mmol) in acetone (20 mL) was added to the mixture of copper(I) chloride (112 mg, 1.13 mmol) and *N*,*N*,*N*′,*N*′-tetramethylethylenediamine (125 mg, 1.08 mmol) in acetone (10 mL). Oxygen was bubbled through the mixture while it was refluxed for 20 h. Solvent of the reaction mixture was evaporated and the residue was recrystallized from chloroform–methanol mixture to give 2.35 g (76%) of 9-BCMU as colorless solid: Mp. 77°C; ^{1}H NMR (400 MHz, $CDCl_3$, δ), 0.94 (6H, t, J = 7.6 Hz), 1.22–1.44 (24H, m), 1.51 (4H, tt, J = 7.2, 7.2 Hz), 1.56–1.69 (8H, m), 2.24 (4H, t, J = 6.9 Hz), 3.96 (4H, d, J = 5.5 Hz), 4.07 (4H, t, J = 6.6 Hz), 4.16 (4H, t, J = 6.9 Hz), 5.17 (2H, broad t); ^{13}C NMR (100 MHz, $CDCl_3$, δ) 13.62, 18.99, 19.14, 25.74, 28.26, 28.75, 28.89, 28.95, 29.15, 29.28, 30.49, 42.65, 65.19, 65.26, 65.42, 77.47, 156.57, 170.21; Found: C, 66.65%; H, 9.38%; N, 4.20%; Calcd for $C_{36}H_{60}N_2O_8$: C, 66.64%; H, 9.32%; N, 4.32%.

The solvents acetone, 1,2-dichloroethane, acetonitrile, tetrahydrofuran (THF), dichloromethane (DCM), diethyl ether, and methyl acetate were purchased from Wako Chemicals with 99% purity or greater, and used without further purification.

Ribbons were grown on glass microscope slides. While surface treatment can often have a significant effect on the growth of crystals, the DCHD ribbon growth was robust: a test in which the glass substrates were washed twice with acetone, twice with distilled water, and treated with ozone plasma for 20 min prior to the sample deposition had no effect on the growth of the ribbons.

Acetone solutions of the DA monomers were made at concentrations of 0.5 mM unless otherwise noted. The CESA method was used to create oriented ribbons of the DA monomer. In this method, a 2.0 mm glass rod was lightly clamped onto a glass substrate. Thirty microliters of the solution was deposited at the interface between the rod and the substrate. Capillary forces pulled the liquid to the edges of the rod and

https://doi.org/10.1557/mrc.2018.201 Published online by Cambridge University Press

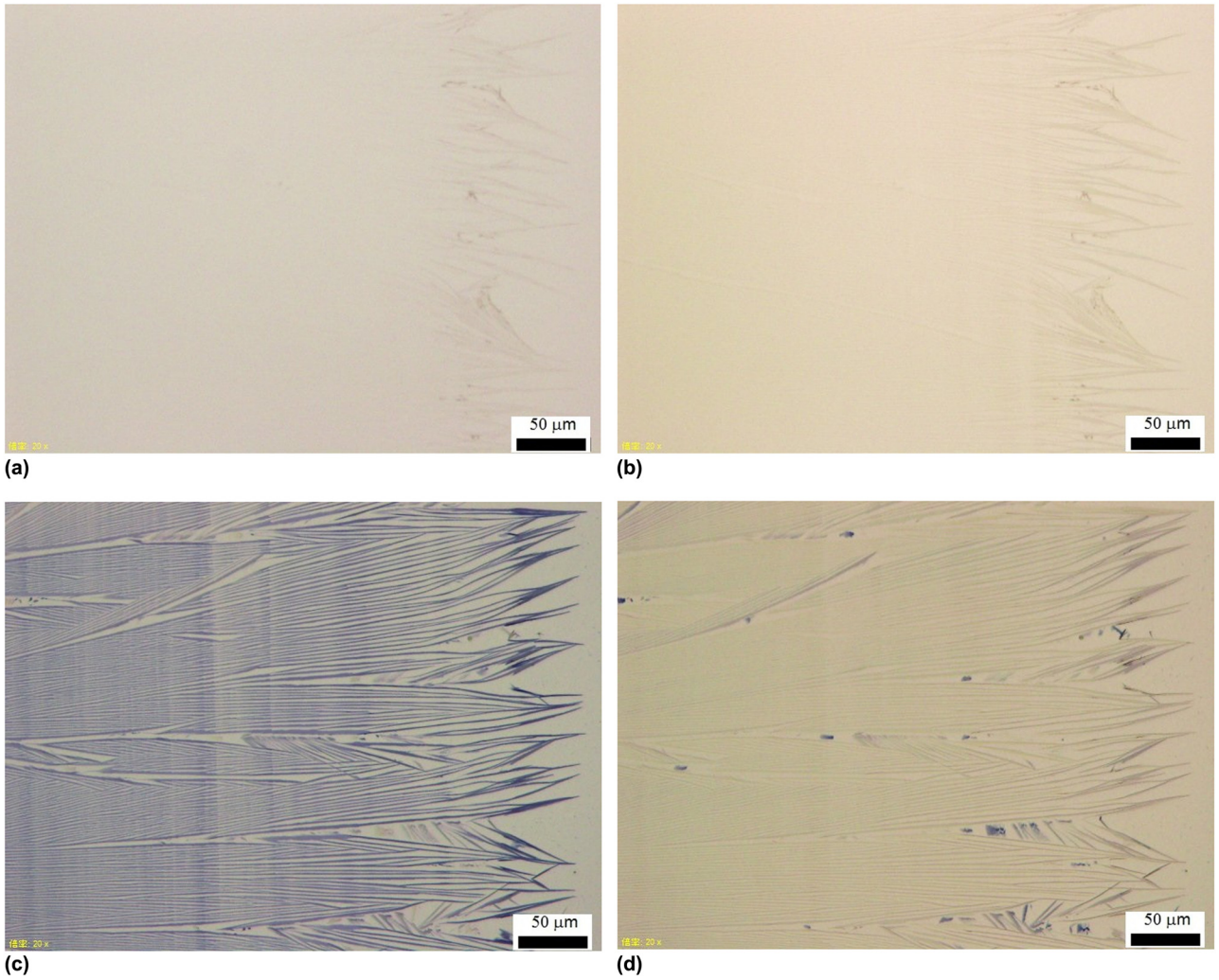


Figure 2. Images of DCHD and poly(DCHD) ribbons; (a) DCHD ribbons (before polymerization) with incident polarization parallel to the long ribbon axis; (b) DCHD ribbons with incident polarization perpendicular to the long ribbon axis; (c) poly(DCHD) ribbons (after polymerization) with incident polarization parallel to the long ribbon axis; (d) poly(DCHD) ribbons with incident polarization perpendicular to the long ribbon axis. The motion of the contact line was from left to right.

substrate. For the acetone solutions, the samples were allowed to dry for 5 min, while for less volatile solvents the drying time was extended to 15 min. Following the drying step, the glass rod was removed and the samples were polymerized. Polymerization was done using UV irradiation with a central wavelength of 254 nm and an irradiance of approximately 1550 W/m^2.

Optical images were taken using an Olympus BX51 in transmission mode. Powder x-ray diffraction patterns were measured using a Bruker D8 Advance diffractometer using Cu K_α radiation (wavelength $\lambda = 1.5418$ Å). Scanning electron microscopy (SEM) images were taken using a JEOL JSM-6700F instrument. Samples were coated with a thin layer of Pt prior to SEM imaging. UV-Vis absorption spectra were measured with a Cary 5000 UV-Vis-NIR spectrophotometer in transmission mode. Atomic force microscopy (AFM) images were collected using an NT-MDT NTEGRA Prima AFM in tapping mode.

Results and discussion

Optical images showed the formation of ribbons of the DCHD monomer, with ribbon widths between 1 and 2 µm and similar values for the distance between ribbons. This is not surprising; it has been shown that the dispersions of poly(DCHD) nanofibers (NFs) can be created using the reprecipitation method.[17,18] The length of the individual ribbons was on the order of 100s of micrometers, giving the aspect ratios of 50–100. After polymerization, the ribbons become much clearer in the images, but only when the polarization of the incident light was parallel to the axis of the ribbons, displaying a large amount of anisotropy, as shown in Fig. 2. The size and separation of the ribbons remained after polymerization. The ribbons were much thinner

https://doi.org/10.1557/mrc.2018.201 Published online by Cambridge University Press

than wide: AFM scans showed thicknesses on the order of 40–70 nm (Supplementary Fig. S1). The ribbons extended over a region of approximately 1 mm. Significant branching of the ribbons was observed, similar to the case when ribbons are formed from molecular charge transfer crystals.[5] Despite the branching and terminations, the ribbons display a relatively narrow range of widths and approximately regular spacing. This has been attributed to the effects of Marangoni flow in cylinders perpendicular to the receding contact line, which transports and deposits material into these regularly spaced regions.[19,20] The DCHD monomers in this case crystallized with the *b*-axis coinciding with the ribbon axis, and can be easily converted to polymer through UV irradiation.[21] SEM images (Supplementary Fig. S2) confirmed the size and structure of the poly(DCHD) ribbons.

Powder x-ray diffraction measurement of the samples, shown in Fig. 3, displayed peak characteristics of poly (DCHD).[22,23] XRD data for PDA are given in the Supplementary material (Fig. S3) for PDA NFs, PDA bulk crystal, and DA crystals. The three diffraction peaks at $2\theta =$ 7°, 11°, and 14° in Fig. 3 are almost the same as those of PDA NFs within experimental error. The peak at $2\theta = 14°$ in Fig. 3 is strong, relative to others, due to the anisotropic orientation of the PDA ribbons. The broad diffraction peak from 20° to 30° is likely due to the glass substrate (Supplementary material Fig. S4). The (111) diffraction peak (not observed) may be embedded in the amorphous peak originating from the glass substrate.

The UV-Vis absorption spectrum of the poly(DCHD) ribbons shown in Fig. 4 displays the absorption in the 500–700 nm range characteristic of PDA, including the excitonic absorption peak at 650 nm, which was somewhat smaller than in bulk, fully polymerized crystals of poly(DCHD).[24] The ribbons also showed a large degree of orientation. This led to a strong linear dichroism, as seen in the figure, with a value for the dichroic ratio $D = \alpha_{\parallel}/\alpha_{\perp}$ of 9.5 at the excitonic

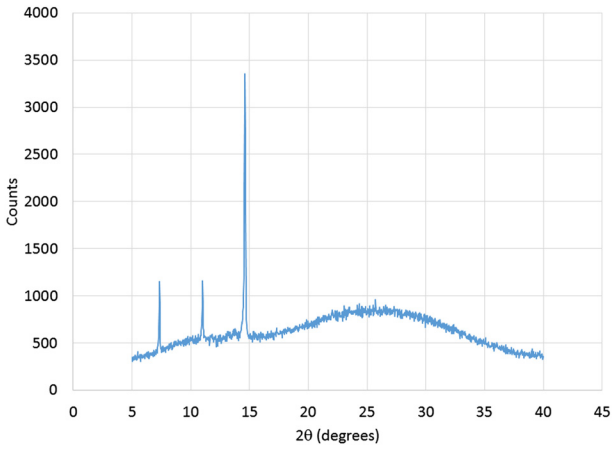


Figure 3. Powder XRD of a poly(DCHD) ribbon film.

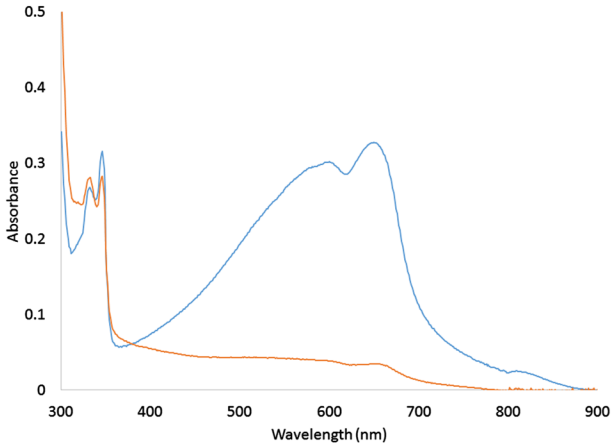


Figure 4. Absorption spectra of poly(DCHD) ribbons. Blue curve: polarization parallel to the long ribbon axis, orange curve: polarization perpendicular to the long ribbon axis.

absorption peak ($\lambda = 650$ nm), giving a value for the order parameter

$$S = \frac{D-1}{D+2} \tag{1}$$

equal to 0.74. Some level of disorder can clearly be seen in the image in Fig. 2, which would explain the value of the order parameter. This disorder may be due to interactions of the DCHD monomer with the surface of the glass substrate.

The concentration of the DCHD monomer had a significant effect on the structure of the resulting poly(DCHD) ribbons. Increasing the concentration induces regions in the films near the initial location of the contact line that contained thick ribbons that were almost continuous, i.e., with very small spacing between the ribbons (see Fig. 5). These were followed by regions that resembled those found in the lower concentration samples. It is likely that the large deposit of solid material at the start of the process results in a drop in the solute concentration, leading to the similar structures.

Decreasing the concentration led to little changes in the widths of the ribbons, but in larger spacing between them (Supplementary Fig. S5). Decreasing concentration also led to lower orientational order, greater curvature in individual poly(DCHD) ribbons, and less regular spacing between them.

The largest effect on the formation of the poly(DCHD) ribbons was due to the solvent. Models have been developed that predict the length scales of the Marangoni flow, which dictates the pattern of deposition of the monomer.[19,20] These length scales depend on solvent parameters such as viscosity and thermal diffusivity as well as temperature gradients across the solution. Acetone seems to be an ideal solvent for ribbon formation at room temperature; numerous other solvents showed no ribbon formation, although the monomer is crystallized and could be polymerized, as shown in Fig. 6.

https://doi.org/10.1557/mrc.2018.201 Published online by Cambridge University Press

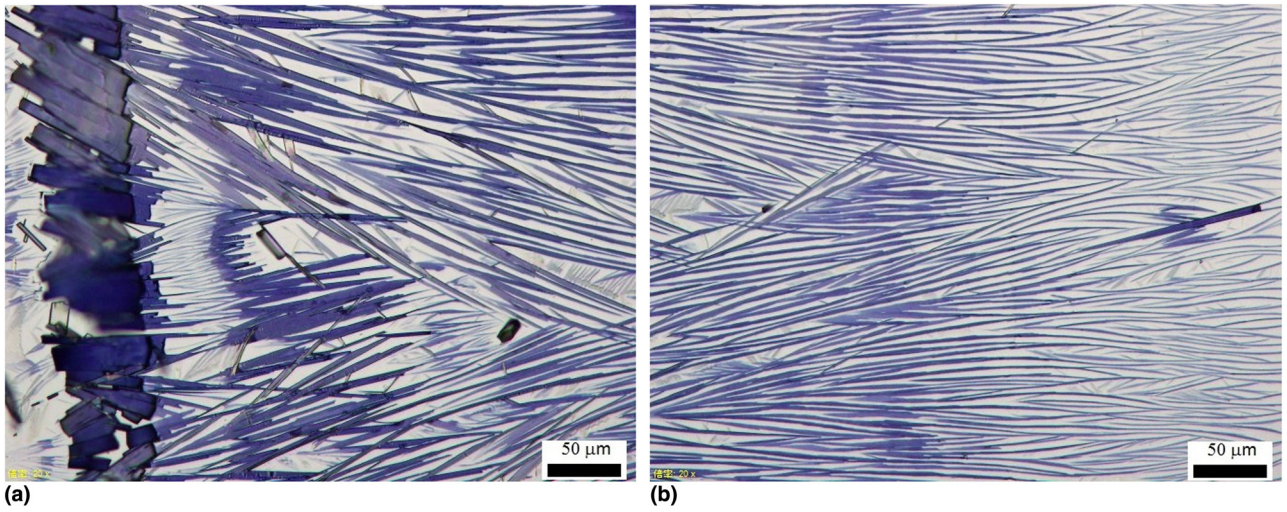


Figure 5. Two regions of a 10.3 mM sample; (a) near the position of the initial contact line; (b) near the glass rod (end of ribbon growth). The motion of the contact line was from left to right.

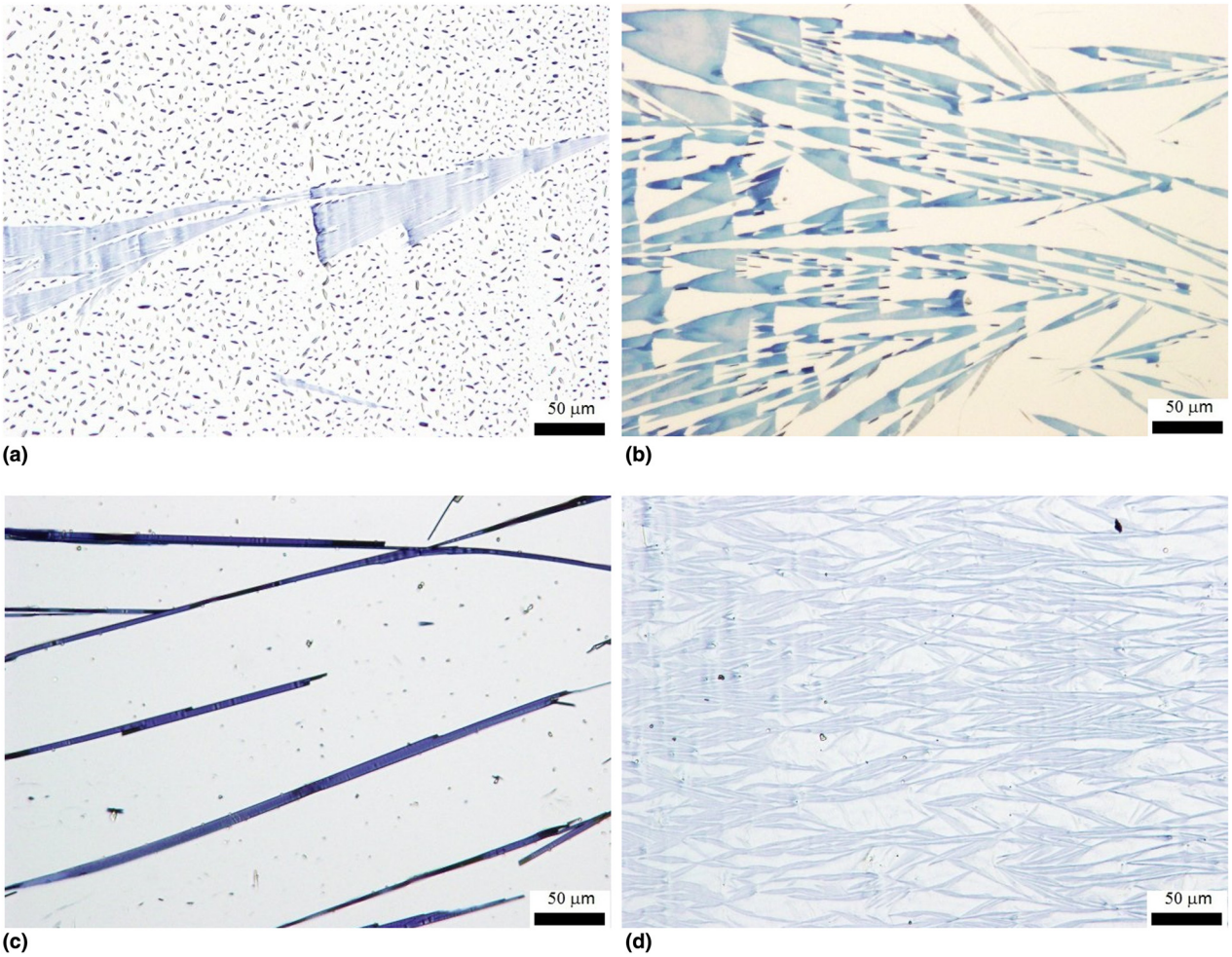


Figure 6. Poly(DCHD) prepared from solutions in (a) DCM, (b) 1,2-dichloroethane, (c) THF, and (d) diethyl ether. The motion of the contact line was from left to right.

https://doi.org/10.1557/mrc.2018.201 Published online by Cambridge University Press

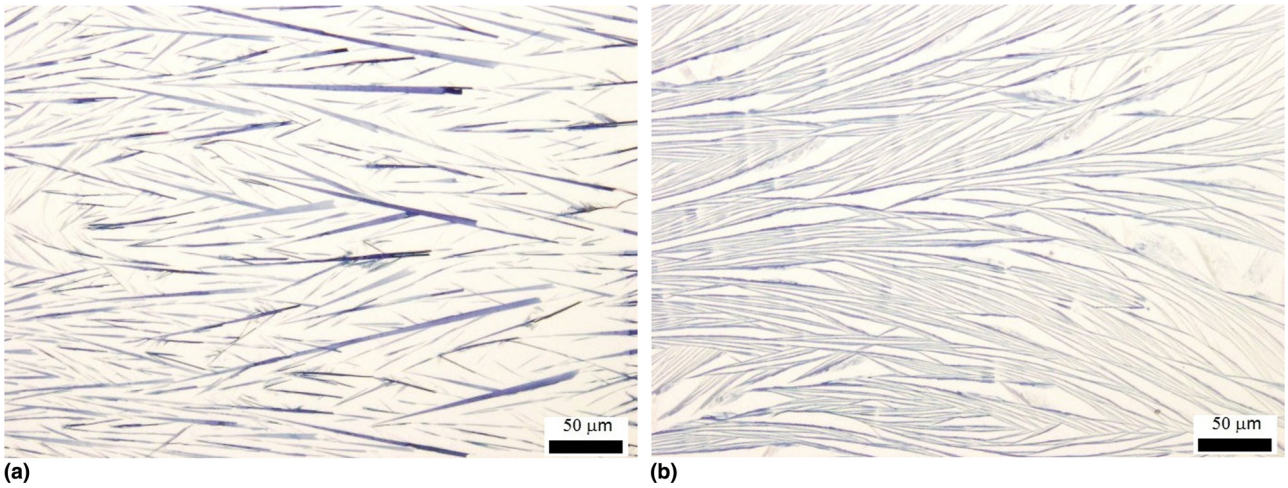


Figure 7. Poly(DCHD) ribbons prepared from acetonitrile (a) and methyl acetate (b). The motion of the contact line was from left to right.

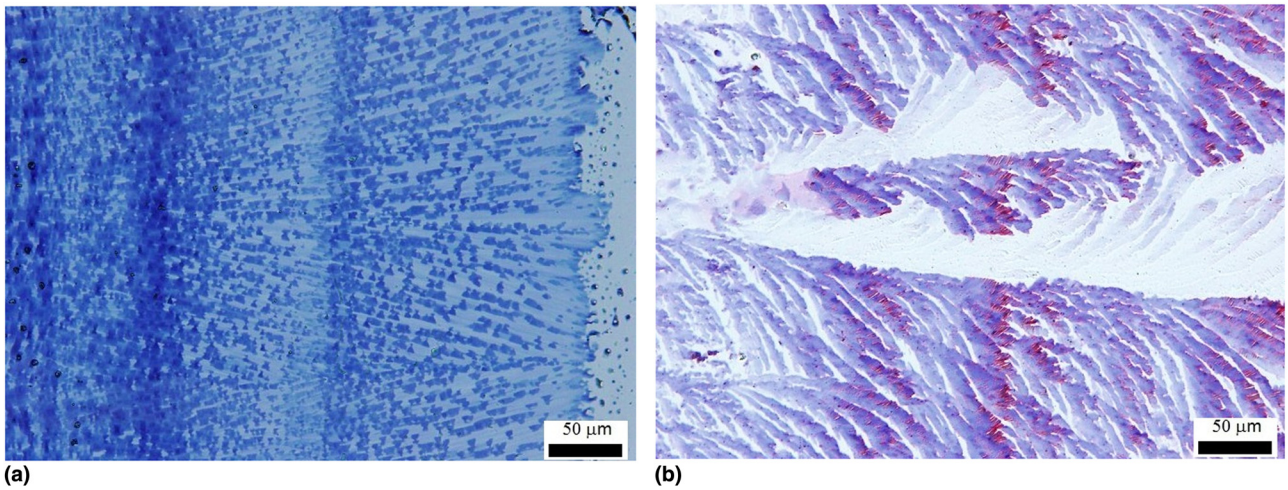


Figure 8. Optical images of poly(9-BCMU) (a) and poly(TCDA) (b). The motion of the contact line was from left to right.

Samples prepared from acetonitrile and methyl acetate, which had viscosities and thermal diffusivities close to those of acetone, were closest in terms of ribbon morphology, as seen in Fig. 7.

Ribbons of other types of PDAs could not be produced. Figure 8 shows the images of poly(9-BCMU) and poly (TCDA). Crystals of the 9-BCMU and TCDA monomer did form, and could be subsequently polymerized. However, while structures formed during CESA showing some effect from the receding contact line and Marangoni effect, the individual ribbons that were observed for poly(DCHD) did not form in poly(9-BCMU) or poly(TCDA). The DPBD only formed an amorphous sheet, which did not display the color changes associated with solid-state polymerization, although DPBD is known to form stable crystals.[21,25] The poly (TCDA) showed both the blue and red phases.[26] Although ribbons were not obtained, there was a considerable degree of orientation, as characterized by optical dichroism. We surmise that the intermolecular packing interaction between DA monomers is stronger than the interaction with the substrate, so that the polymerizable-ordered crystal state is formed during the CESA process. The ability of poly(DCHD) to form good ribbons is likely due to the side group further stabilizing the monomer self-assembly.[18]

Conclusions

We have shown that the method of CESA can be used to create oriented ribbons of a DA monomer, which can then be

https://doi.org/10.1557/mrc.2018.201 Published online by Cambridge University Press

polymerized in the solid state to give ribbons of the PDA, i.e., poly(DCHD). The ability to create these ribbons was sensitive to both the monomer structure and the solvent used. This method may be useful for producing structures which could easily be incorporated into devices such as organic field effect transistors.

Supplementary Material Available: AFM measurements of ribbon thickness, SEM images of polymer ribbons, PXRD spectra of bulk and nanocrystal polymers, PXRD of the substrate, optical images of ribbons formed at different concentrations.

Supplementary Material

The supplementary material for this article can be found at https://doi.org/10.1557/mrc.2018.201

References

1. J.W. Ward, Z.A. Lamport, and O.D. Jurchescu: Versatile organic transistors by solution processing. *Chem. Phys. Chem.* **16**, 1118 (2015).
2. C. Sekine, Y. Tsubata, T. Yamada, M. Kitano, and S. Doi: Recent progress of high performance polymer OLED and OPV materials for organic printed electronics. *Sci. Technol. Adv. Mater.* **15**, 034203 (2014).
3. X. Gao and Z. Zhao: High mobility organic semiconductors for field-effect transistors. *Sci. China-Chem.* **58**, 947 (2015).
4. B.B. Patel and Y. Diao: Multiscale assembly of solution-processed organic electronics: the critical roles of confinement, fluid flow, and interfaces. *Nanotechnology* **29**, 044004 (2018).
5. S. Bi, Z. He, J. Chen, and D. Li: Solution-grown small-molecule organic semiconductor with enhanced crystal alignment and areal coverage for organic thin film transistors. *AIP Adv.* **5**, 077170 (2015).
6. W. Han, M. Byun, L. Zhao, J. Rzayev, and Z. Lin: Controlled evaporative self-assembly of hierarchically structured bottlebrush block copolymer with nanochannels. *J. Mater. Chem.* **21**, 14248 (2011).
7. N. Liu, Y. Zhou, L. Wang, J. Peng, J. Wang, J. Pei, and Y. Cao: In situ growing and patterning of aligned organic nanowire arrays via dip coating. *Langmuir* **25**, 665 (2009).
8. H. Nakanishi and H. Kasai: Polydiacetylene microcrystals for third-order nonlinear optics. *ACS Symp. Ser.* **672**, 183 (1997).
9. H. Oikawa: Hybridized organic nanocrystals for optically functional materials. *Bull. Chem. Soc. Jpn.* **84**, 233 (2011).
10. M. Camacho, A. Kar, B. Wherrett, M. Bakarezos, R. Rangel-Rojo, S. Yamada, H. Matsuda, H. Kasai, and H. Nakanishi: All-optical switching potentiality in Fabry-Perot devices containing poly-DCHD. *Opt. Commun.* **251**, 376 (2005).
11. J. Lee, A. Aleshin, D. Kim, H. Lee, Y. Kim, G. Wegner, V. Enkelmann, S. Roth, and Y. Park: Field-effect mobility anisotropy in PDA-PTS single crystals. *Synth. Met.* **152**, 169 (2005).
12. J. Nishide, T. Oyamada, S. Akiyama, H. Sasabe, and C. Adachi: High field-effect mobility in an organic thin-film transistor with a solid-state polymerized polydiacetylene film as an active layer. *Adv. Mater.* **18**, 3120 (2006).
13. G. Zou, E. Lim, R. Tamura, N. Kajimoto, T. Manaka, and M. Iwamoto: Surface morphology and electrical transport properties of polydiacetylene-based organic field-effect transistors. *Jpn. J. Appl. Phys.* **45**, 6436 (2006).
14. T. Koyanagi, M. Muratsubaki, Y. Hosoi, T. Shibata, K. Tsutsui, Y. Wada, and Y. Furukawa: Organic field-effect transistor based on a thin film of polydiacetylene prepared from 10,12-pentacosadiynoic acid. *Chem. Lett.* **35**, 20 (2006).
15. G. Wegner: Topochemical reactions of monomers with conjugated triple-bonds. IV. Polymerization of bis-(p-toluene sulfonate) of 2.4-hexadiin-1.6-diol. *Makromol. Chem.* **145**, 85 (1971).
16. D.J. Sandman, L.A. Samuelson, and C.S. Velazquez: Synthesis and solid-state polymerization of urethane-substituted diacetylene monomers of improved purity. *Polym. Commun.* **27**, 242 (1986).
17. T. Onodera, T. Oshikiri, H. Katagi, H. Kasai, S. Okada, H. Oikawa, M. Terauchi, M. Tanaka, and H. Nakanishi: Nano-wire crystals of pi-conjugated organic materials. *J. Cryst. Growth.* **229**, 586 (2001).
18. Y. Iimori, T. Onodera, H. Kasai, M. Mitsuishi, T. Miyashita, and H. Oikawa: Fabrication of pseudo single crystalline thin films composed of polydiacetylene nanofibers and their optical properties. *Opt. Mater. Express.* **7**, 2218 (2017).
19. M. Maillard, L. Motte, A. Ngo, and M. Pileni: Rings and hexagons made of nanocrystals: a Marangoni effect. *J. Phys. Chem. B.* **104**, 11871 (2000).
20. H. Ma, R. Dong, J.D. Horn, J. Hao, and J.D. Van Horn: Spontaneous formation of radially aligned microchannels. *Chem. Commun.* **47**, 2047 (2011).
21. V. Enkelmann: Structural aspects of the topochemical polymerization of diacetylenes. *Adv. Polym. Sci.* **63**, 91 (1984).
22. K. Tashiro, H. Nishimura, and M. Kobayashi: First success in direct analysis of microscopic deformation mechanism of polydiacetylene single crystal by the x-ray imaging-plate system. *Macromolecules* **29**, 8188 (1996).
23. H.R. Chung, E. Kwon, H. Oikawa, H. Kasai, and H. Nakanishi: Effect of solvent on organic nanocrystal growth using the reprecipitation method. *J. Cryst. Growth.* **294**, 459 (2006).
24. R. Hood, H. Muller, C. Eckhardt, R. Chance, and K. Yee: Optical-properties of a polydiacetylene crystal—poly-[1,6-Di(N-carbazolyl)-2,4-hexadiyne]. *Chem. Phys. Lett.* **54**, 295 (1978).
25. E.H. Wiebanga: The crystal structure of diphenyldiacetylene. C_6H_5 C=C-C=C-C_6H_5. *Z. Kristallogr.* **102**, 193 (1940).
26. B. Tieke, D. Bloor, and R. Young: Solid-state polymerization of tricosa-10,12-diynoic acid. *J. Mater. Sci.* **17**, 1156 (1982).

https://doi.org/10.1557/mrc.2018.201 Published online by Cambridge University Press